TAL1 cooperates with PI3K/AKT pathway activation in T-cell acute lymphoblastic leukemia

Naomi Thielemans,[1,2,3] Sofie Demeyer,[1,2,3] Nicole Mentens,[1,2,3] Olga Gielen,[1,2,3] Sarah Provost[1,2,3] and Jan Cools[1,2,3]

[1]Center for Human Genetics, KU Leuven; [2]Center for Cancer Biology, VIB and [3]Leuven Cancer Institute (LKI), KU Leuven – UZ Leuven, Leuven, Belgium

Correspondence: J. Cools
jan.cools@kuleuven.be

Received: July 28, 2021.
Accepted: March 22, 2022.
Prepublished: March 31, 2022.

https://doi.org/10.3324/haematol.2021.279718

©2022 Ferrata Storti Foundation
Haematologica material is published under a CC BY-NC license

Abstract

TAL1 is ectopically expressed in about 30% of T-cell acute lymphoblastic leukemia (T-ALL) due to chromosomal rearrangements leading to the STIL-TAL1 fusion genes or due to non-coding mutations leading to a *de novo* enhancer driving TAL1 expression. Analysis of sequence data from T-ALL cases demonstrates a significant association between TAL1 expression and activating mutations of the PI3K-AKT pathway. We investigated the oncogenic function of TAL1 and the possible co-operation with PI3K-AKT pathway activation using isogenic pro-T-cell cultures *ex vivo* and *in vivo* leukemia models. We found that TAL1 on its own suppressed T-cell growth, in part by affecting apoptosis genes, while the combination with AKT pathway activation reduced apoptosis and was strongly driving cell proliferation *ex vivo* and leukemia development *in vivo*. As a consequence, we found that TAL1+AKT^{E17K} transformed cells are more sensitive to PI3K-AKT pathway inhibition compared to AKT^{E17K} transformed cells, related to the negative effect of TAL1 in the absence of activated PI3K-AKT signaling. We also found that both TAL1 and PI3K-AKT signaling increased the DNA-repair signature in T cells resulting in synergy between PARP and PI3K-AKT pathway inhibition. In conclusion, we have developed a novel mouse model for TAL1+AKT^{E17K} driven T-ALL development and have identified a vulnerability of these leukemia cells to PI3K-AKT and PARP inhibitors.

Introduction

T-cell acute lymphoblastic leukemia (T-ALL) is an aggressive disease and symptoms are mostly caused by high proliferation of leukemic blasts in the bone marrow, leading to failure of normal hematopoiesis. Treatment of T-ALL remains a challenge. Although children have a good prognosis and a high chance of overall survival, this comes with important treatment toxicity leading to both short- and long-term side effect.[1] Furthermore, adults and children with resistant or relapsed disease are often incurable. Therefore, further understanding of the pathogenesis of T-ALL can lead to identification of new and specific therapeutic targets which can improve the survival and quality of life of these patients.

Based on gene expression profiling and molecular genetic analysis, T-ALL cases were initially classified into five major subgroups.[2,3] Homminga *et al.* identified an additional subgroup represented by aberrant expression of *NKX2-1*.[4] Genomic characterization based on whole-exome sequencing and RNA sequencing on 264 T-ALL samples defined eight different subgroups based on genomic rearrangements and/or ectopic expression of one specific transcription factor: *TAL1*, *TAL2*, *TLX1*, *TLX3*, *HOXA*, *LMO1/LMO2*, *LMO2/LYL1* and *NKX2-1*.[5] In these classifications, each subgroup correlates to a differentiation arrest at specific stages of normal T-cell development.[3]

In up to 30% of T-ALL patients *TAL1* expression is reactivated via various mechanisms, including translocation, deletion, or non-coding mutations creating a *de novo* enhancer region close to TAL1.[6,7] TAL1 belongs to the class II basic helix-loop-helix (bHLH) transcription factors which obligatory dimerizes with class I bHLH transcription factors called E proteins (E2A, HEB E and E2-proteins). TAL1 is known to play an important role in the regulation of normal embryonic and adult hematopoiesis, but is silenced during normal T-cell development.[8]

Despite numerous studies on the function of TAL1 and its known transcriptional activities in hematopoietic progenitor cells, the exact mechanism by which TAL1 is impli-

cated in T-ALL development is still poorly characterized. A first transgenic mouse models with *TAL1* expression under control of the T-cell specific *LCK* promotor developed T-cell malignancy with a very long latency and low penetrance,[9] and *TAL1* expression under control of lymphoid specific CD2 promotor did not cause any disease.[10] These findings suggested that additional mutations were needed in addition to *TAL1* expression to cause T-cell malignancy. Subsequently, several mouse models were developed that focused on the potential cooperation between *TAL1* and *LMO1* or *LMO2* expression, because co-expression between *TAL1* and *LMO1* or *LMO2* was reported in human T-ALL.[11] These models were successful and Larson *et al*. reported leukemia development in a *Tal1/Lmo2* transgenic mice and Tatarak *et al*. reported rapid development of T-ALL upon thymic expression of *Tal1* and *Lmo1*.[12-13] Moreover, in the majority of the leukemias spontaneous mutations in *Notch1* were identified. Tremblay and colleagues generated *Notch1/Tal1/Lmo1* triple transgenic mice and reported that these animals developed leukemia with shorter latency compared to single or double transgenic animals.[14] CD4/CD8 double negative cells from *Notch1/Tal1/Lmo1* triple transgenic mice were able to induce T-ALL in secondary recipient animals with high efficiency compared with *Tal1/Lmo1* double transgenic mice. A subsequent study further suggested that *Notch1* drives self-renewal of thymocytes from the *Tal1/Lmo1* mouse model via its target genes *Hes1* and *Myc*.[15]

However, despite leukemia development in these elegant mouse models, more complete genomic and transcriptomic data on T-ALL have not supported an important role for deregulated *LMO1* or *LMO2* expression in *TAL1* positive T-ALL. In contrast, it has become clear that *PTEN* deletion and variant mutations leading to PI3K-AKT pathway activation are very common in *TAL1* expressing T-ALL, while these are less frequent in the other T-ALL subgroups.[6,16-18] We present here novel *in vivo* and *ex vivo* mouse models for TAL1/AKT driven T-ALL development and use these models to identify novel vulnerabilities in these leukemias.

Methods

Laboratory animals and mouse bone marrow transplantation assays

All mice were monitored daily and housed in individually ventilated cages cages in specific pathogen free (SPF) or semi-SPF conditions in the KU Leuven animal facility. Mouse experiments were approved and supervised by the KU Leuven ethical committee (ECD P013/2018).

Bone marrow transplantation was performed with hematopoietic stem/progenitor cells harvested from male rosa26 CD2cre C57BL/6 mice. These cells were transduced with retroviral vectors for expression of the genes of interest, with MSCV-based vectors giving constitutive expression or inducible expression based on inversion of a floxed region in the viral vector as described previously.[19] Cells were injected via tail vein injection into sublethal irradiated (5Gy) female recipients C57BL/6 mice. Leukemia development was followed by blood collection from the facial vein every 2 weeks. Secondary and tertiary transplants were performed through injection of malignant cells via tail vein into irradiated (2.5 Gy) female recipients C57BL/6 mice recipient mice. Mice were sacrificed when white blood cell count was over 25,000/µL, when they lost 10% of initial weight or other signs of severe morbidity.

Primary mouse pro-T-cell cultures

Pro-T cell cultures were established as described.[18,20] Hematopoietic stem and progenitor cells (HSPC) were isolated from Rosa26-CreER knockin or Cas9 knockin transgenic mice. CreER cells have a tamoxifen-inducible Cre-mediated recombination system,[21] while the Cas9 cells were used to inactivate genes with guide RNA, as described previously.[22] Pro-T cells were cultured on DLL4-coated plates in RPMI media containing 20% fetal bovine serum (FBS), primocin (100 µL/mL), IL7 and SCF (both 20 ng/mL). Pro-T cells were spinfected with retroviral constructs. Growth was followed over time by measuring growth density and percentage of fluorescent cells.

Western blotting

Cells were lysed in cold lysis buffer containing 5 mM Na_3VO_4 and protease inhibitors (complete EDTA-free), antibodies used for western blotting: TAL1 (Santa Cruz-393287), p-AKT (CST Ser473 D9E 4060); AKT (Thermo MA5-14916), p-GSK3β (CST 5558), GSK3β (Merck Milipore 05-412), β-Actin (Sigma Aldrich A5441). Secondary antibodies: anti-rabbit IgG (CST 7074), anti-mouse IgG (Cytiva, NA931).

RNA-sequencing and analysis

RNA was extracted from tissue and cells using the Maxwell 16 LEV Simply RNA purification kit (Promega). Next-generation sequencing libraries were constructed from 500 ng of total RNA, using the Truseq RNA sample prep kit v2 (Illumina) and subjected to 150 bp single-end sequencing on a HiSeq 4000 instrument (Illumina). The sequencing data was then processed with our in-house pipeline, which consist of cleaning the data with fastq-mcf, performing a quality control with FastQC and mapping to the *Mus musculus* reference genome (mm10) with HISAT2. Subsequently, htseq-count was applied to count the number of reads per gene and a differential gene expression analysis was performed with the R-package DESeq2. The output of this DESeq2 algorithm was used to construct ranked gene lists with a ranking value calcu-

lated as -sign($\log_2$FC)*log(padj). Ranked gene set enrichment analyses were performed with the BROAD gene set enrichment analysis (GSEA) software. Multiple gene sets were used, such as the KEGG pathway database, the hallmark gene sets from MSigDB, and several in-house gene sets.

Drug treatment experiments

Different T-ALL cell lines (both TAL1 positive and TAL1 negative) were cultured in RPMI containing 20% FBS. For drug treatment, cells were seeded at 1-4x10^5 cells/mL in 96 well plates (100 µL/well). Pro-T cells were cultured as described above and seeded at 5x10^5 cells/mL in 96 well plates (100 µL/well). Leukemia mouse thymus cells were cultured *ex vivo* in RPMI containing 20% FBS with IL7, stem cell factor and primocin and seeded at 3x10^3cells/mL in 96 well plates (100 µL/well). Dactoslibib, MK-2206 or dimethyl sulfoxide (Sigma Aldrich), Olaparib (MedChemExpress) were dispensed at the desired concentrations using a Tecan D300e Digital Dispenser. Experiments were performed as biological triplicates. Cell viability was measured after 48 hours (h) (cellines) or 24 h (pro-T cells and thymic cells) of drug treatment with the ATPlite Luminescence Assay System kit (PerkinElmer) on a VICTOR Multilabel Plate Reader (PerkinElmer).

Statistics and other methods

The statistical analysis were performed using Graphad Prism 8. Results were considered statistically significant at $P<0.05$. The appropriate statistical test are specified in the figure legends. Limiting dilution analysis of mouse leukemia cells was calculated using the free ELDA software (https://bioinf.wehi.edu.au/software/elda/).[23]

Results

TAL1-positive T-cell acute lymphoblastic leukemia patients frequently harbor hyperactivating mutation of the PI3K pathway

In order to study the role of *TAL1* in T-ALL and its association with other gene expression or mutations, we reanalyzed genomic and transcriptomic data from previous studies. *TAL1* expression is high in up to 30% of T-ALL cases due to chromosomal rearrangements (*STIL-TAL1* fusion or translocations involving *TAL1*) or due to non-coding mutations that create a *de novo* enhancer upstream of the *TAL1* promoter (Figure 1A).[5-7] Historically, studies on *TAL1* have focused on the cooperation between *TAL1* and *LMO2* since initial studies reported rearrangement of both *TAL1* and *LMO2* in (rare) T-ALL samples and *TAL1* is regularly co-expressed with *LMO1* or *LMO2* in T-ALL cell lines.[24-26] However, recent transcriptomic data from large T-ALL cohorts showed that only a minority of *TAL1* positive cases show high expression of *LMO1* or *LMO2*, with only five *TAL1* positive cases harboring a genetic alteration of *LMO2*.[5,27] Overall, expression of *LMO1/LMO2* was not significantly different in the *TAL1* subgroup compared to other subgroups, indicating that no increased expression of *LMO1/LMO2* factors is required in the *TAL1* subgroup (Figure 1A).

Interestingly, several studies have indicated that *TAL1* positive T-ALL cases often harbor *PTEN* deletions.[5,16-17,27-29] We re-analyzed sequencing data from >500 T-ALL patients from Belgian (n=155), Chinese (n=130) and American (n=264) T-ALL cohorts.[5,27,28] In all studies, there was a clear association between *TAL1* expression and activating mutations in the PI3K-AKT pathway (Figure 1B). In contrast, mutations in the JAK-STAT and RAS pathways were found to be rare in *TAL1* positive T-ALL, but more frequent in the other T-ALL subgroups (Figure 1B).

The Liu *et al*. study contains the most complete data on mutations, expression and copy number variation and shows that 55% of all *TAL1* positive cases harbor an activating mutation in the PI3K-AKT pathway (Figure 1B).[5] The majority (69%) of these cases have a deletion, frameshift or nonsense mutation in *PTEN* and other cases have mutations in the PI3K complex or in *AKT1* or *AKT2* genes. Analysis of the expression data of these cases confirmed increased expression of PI3K-AKT pathway associated genes in the cases with *PTEN* inactivation or other PI3K-AKT pathway mutations compared to the *TAL1*-positive cases without such mutations (Figure 1C), indicating stronger PI3K-AKT pathway activation in the *TAL1* cases with PI3K-AKT-PTEN mutations compared to the other *TAL1*-positive cases.

TAL1 cooperates with PI3K activating mutations in driving T-cell acute lymphoblastic leukemia *in vivo*

Here we used a bone marrow transplant model to determine the oncogenic potency of *TAL1* and activated PI3K-AKT signaling (by expressing AKT^{E17K}, an active AKT mutant) alone or in combination to induce T-ALL development *in vivo*.

When using a retroviral vector to constitutively express *TAL1* together with AKT^{E17K} in HSPC of C57BL/6 mice, this led to leukemic disease with variable immunophenotype with both myeloid and lymphoid markers (data not shown). In this way, no T-ALL model could be generated and could reflect the fact that we are not targeting the right cell of origin to obtain T-ALL. In order to overcome this problem, we set up a bone marrow transplant assay using our recently developed Cre-inducible retroviral vector in which oncogene expression can be limited to specific cell types when used in combination with transgenic Cre mice (Figure 2A).[19] In order to get lymphoid-restricted expression of the oncogenes, we isolated HSPC from CD2-Cre mice and transduced these cells with the inducible

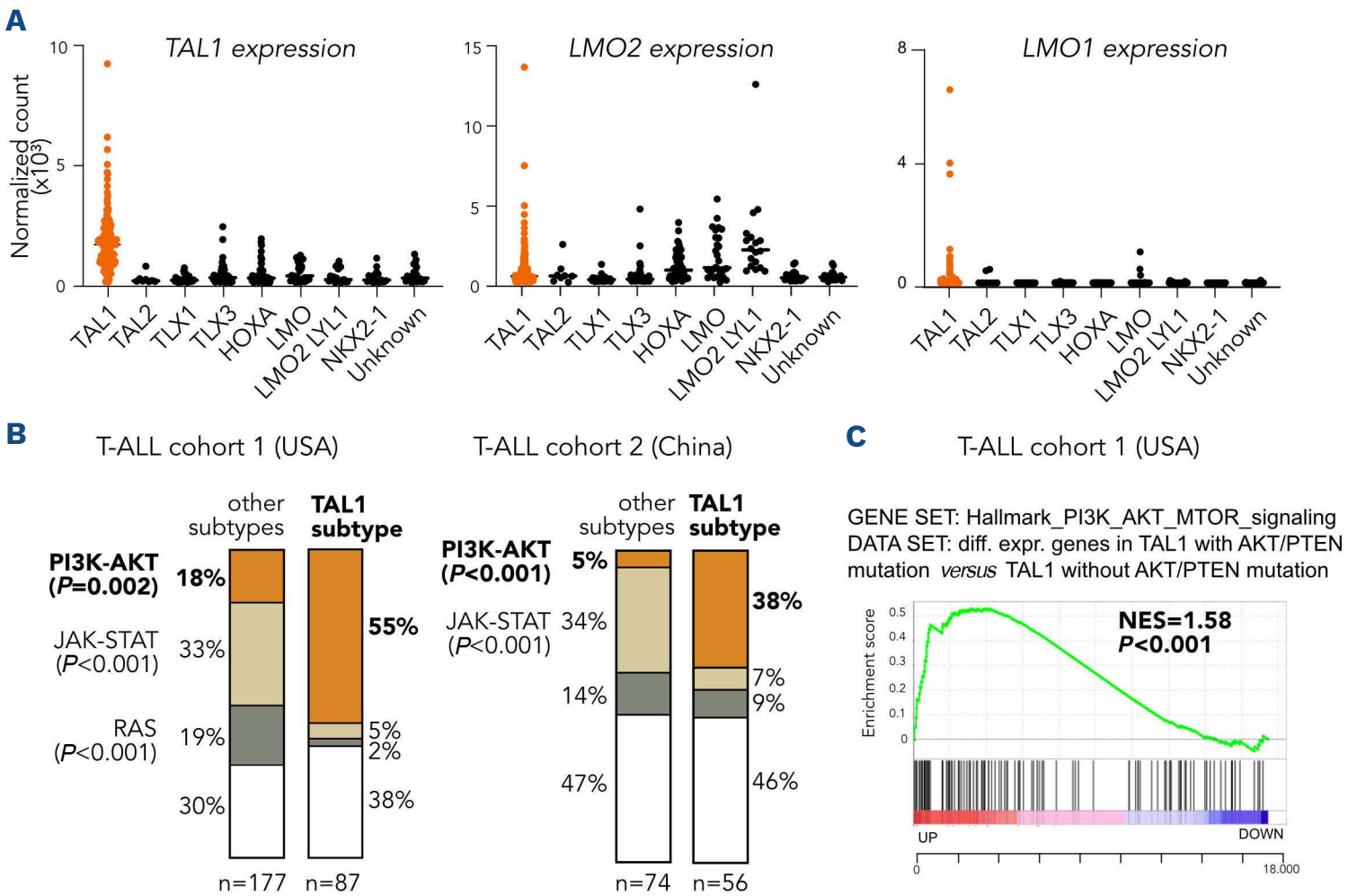

Figure 1. Aberrant expression of *TAL1* co-occurs with PI3K pathway mutations in T-cell acute lymphoblastic leukemia patients. (A) Violin plots showing expression of *TAL1*, *LMO2* and *LMO1* in different T-cell acute lymphoblastic leukemia (T-ALL) patient subgroups (Mullighan data set). (B) Distribution of hyperactivation of signaling pathways in TAL1 and non-TAL1 subgroups in two patient cohorts: (USA) Liu data set 87/264 (33%) and (China) Chen data set 56/130 (43%). Using Fisher's exact test, *P*-values were calculated for testing significance of positive association between TAL1 subgroup and hyperactivation of different pathways. (C) Gene set enrichment analysis showing significant positive enrichment of PI3K pathway in TAL1 patients harboring PI3K-AKT-mTOR pathway mutation compared to TAL1 pathways without associated mutations.

retroviral vectors containing TAL1 or AKT^{E17K} or TAL1+AKT^{E17K}. The transduced cells were injected in sub-lethally irradiated wild-type recipient mice to follow disease development over time (Figure 2A).

Transplantation of TAL1-transduced cells did not cause any disease. In contrast, transplantation of cells expressing AKT^{E17K} alone caused T-cell lymphoblastic lymphoma with an average latency of 83 days (Figure 2B). Expression of TAL1+AKT^{E17K} also caused T-cell lymphoblastic lymphoma with a similar latency as AKT^{E17K} alone (average 89 days). These animals did not show elevated white blood cell count and almost no mice had infiltration of peripheral organs such as blood, spleen, liver and bone marrow (Figure 2C and D; *Online Supplementary Figure S1*). Sporadically, mice had infiltration of leukemic cells in the spleen and bone marrow, but always below 20%. The lymphoma cells were late cortical stage (CD4$^+$CD8$^+$) T cells in both conditions and the disease was oligoclonal as determined by expression of a limited set of variable regions of the T-cell receptors α and β (*Online Supplementary Figure S2*).

Despite the similar disease latency, there were marked differences between TAL1+AKT^{E17K} and AKT^{E17K} driven lymphoma. TAL1 expression was confirmed at protein level in lymphoma cells of TAL1+AKT^{E17K} mice (Figure 2E). Lymphoma cells of the TAL1+AKT^{E17K} condition expressed CD25, a marker of activated T cells, which was absent in AKT^{E17K} lymphoma cells (Figure 2F). Moreover, TAL1+AKT^{E17K} cells showed increased expression of *TRIB2*, a gene known to be implicated in TAL1 positive T-ALL,[30] as well as of *IKZF2* and *LMO4* (Figure 2G).

Strikingly, only the TAL1+AKT^{E17K} lymphoma cells were transplantable to secondary mice and caused leukemia with leukocytosis in secondary recipients, while the AKT^{E17K} lymphoma cells were not transplantable (Figure 3A). Immunophenotype in the secondary recipients was again CD4$^+$CD8$^+$, and white blood cell counts were now elevated in all secondary recipients of TAL1+AKT^{E17K} transformed cells (Figure 3B to D). These data indicate that AKT pathway activation in lymphoid progenitor cells is sufficient to activate proliferation and survival pathways, but that *TAL1* expression is required to induce more stem cell properties. TAL1+AKT^{E17K} lymphoma cells were transplantable to secondary mice even when only 50,000 cells were transplanted, but only rarely when 25,000 cells were transplanted, resulting in an estimate of 1/40,000 leukemia initiating cells (LIC).

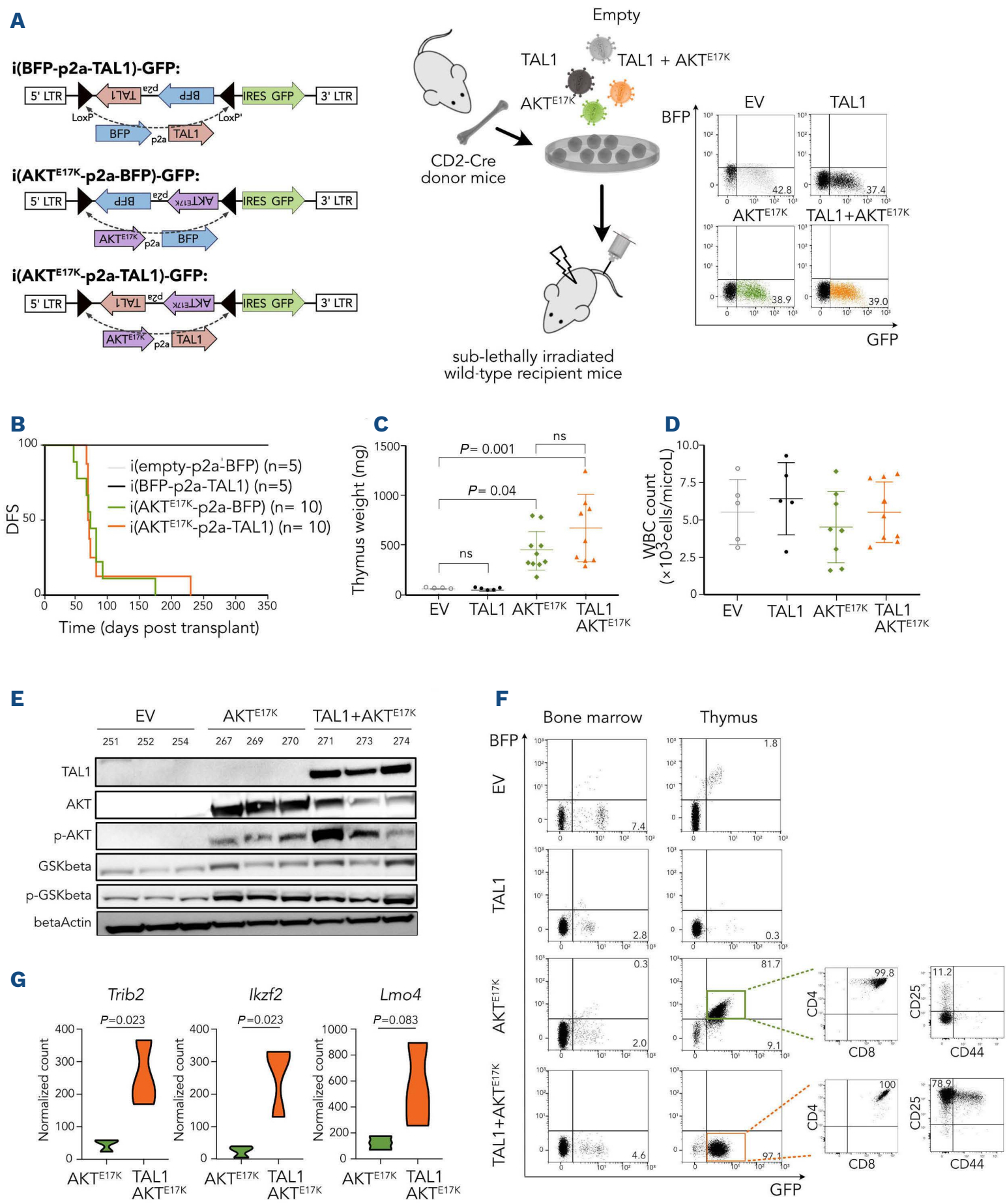

Figure 2. *TAL1* expression and PI3K-AKT activating mutations cooperate in driving T-cell malignancies. (A) Scheme of bone marrow transplantation set-up. We used inducible vectors (indicated as 'i') with constructs of interest initially cloned in antisense orientation flanked by two inverted loxP sites. Hematopoietic stem and progenitor cells (HSPC) were isolated from the bone marrow of CD2-Cre donor mice, followed by retroviral transduction with empty vector (EV), inducible *TAL1*, inducible *AKT^{E17K}* or inducible *TAL1+AKT^{E17K}*. HSPC were checked for transduction efficiencies (based on green fluorescent protein [GFP] that is always expressed; blue fluorescent proteinn [BFP] only becomes expressed in lymphoid cells) but were not sorted prior to injection into irradiated recipient mice. (B) Survival plot showing disease-free survival (DFS) of mice which were primary transplanted with above mentioned constructs *P*-values were calculated with Gehan-Breslow-Wilcoxon test. (C and D) Plots showing thymus weight (C) and white blood cell (D) count at time of sacrifice. *P*-values were calculated using the one-way ANOVA with Tukey correction to account for multiple comparisons. (E) Protein expression of *TAL1* and PI3K pathway components in thymus' cells of sacrificed mice. (F) Flow cytometry analysis of bone marrow and thymus at time of sacrifice- BFP y-axis; GFP x-axis. Thymus lymphoma cells of AKT^{E17K} mice (BFP + GFP double positive) and *TAL1+AKT^{E17K}* (GFP only) were stained for CD8 (APC-eFluor 780, X-axis) and CD4 (PE-Cy7, Y axis) and stained for CD25 (APC, X-axis) and CD44 (PerCP-Cy5, Y-axis). (G) Violin plots showing expression of *Trib2*, *Ikzf2* and *Lmo4* in lymphoma cells of *AKT^{E17K}* and *TAL1-AKT^{E17K}* mice. *P*-values were calculated using unpaired *t*-test.

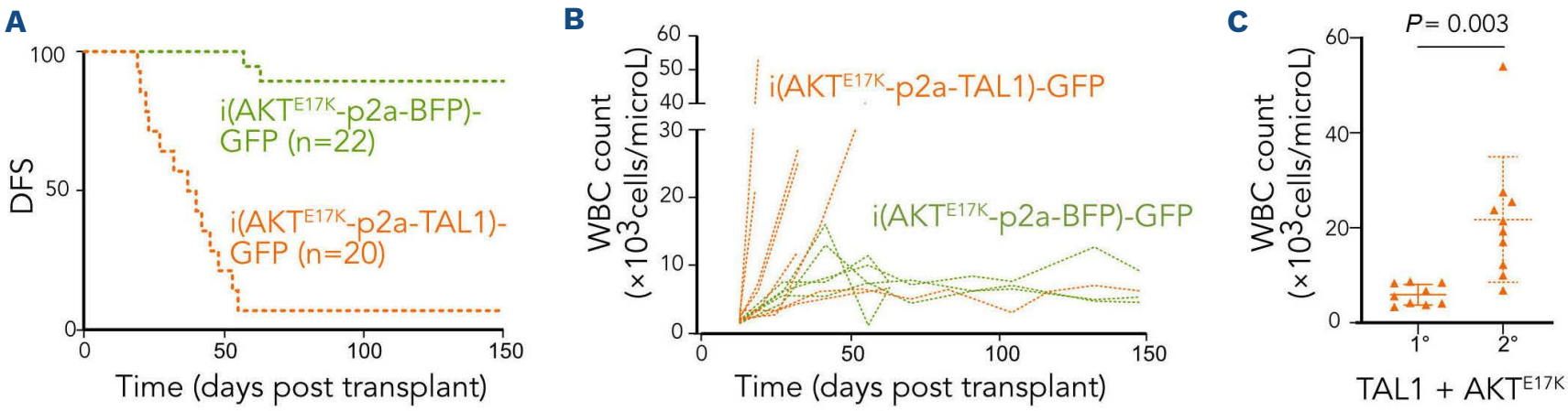

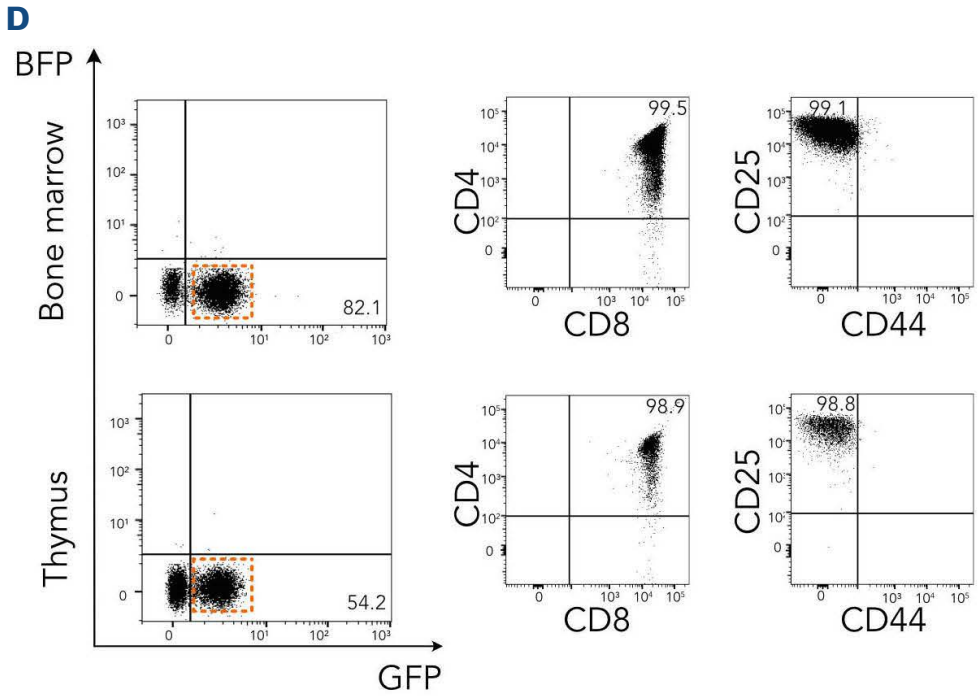

Figure 3. *TAL1-AKT^{E17K}* malignant cells are transplantable. (A) Survival plot showing disease-free survival (DFS) of secondary recipient mice transplanted with thymic lymphoma cells of the primary mouse models. *P*-value was calculated with Gehan-Breslow-Wilcoxon test. (B) White blood cell count of secondary transplanted mice followed over time. (C) White blood cell count of *TAL1-AKT^{E17K}* mice: primary transplantation compared to secondary transplantation. *P*-value was calculated using unpaired *t*-test. (D) Flow cytometry analysis of peripheral blood, bone marrow, spleen and thymus of secondary transplanted mice (m133 – primary m119). Green fluorescent protein (GFP)-positive cells were stained as in Figure 2F.

Expression of *TAL1* in pro-T cells leads to growth disadvantage which can be rescued by AKT^{E17K} or Pten^{del}

In order to study the effects of *TAL1* with and without co-expression of AKT^{E17K} we used *ex vivo* mouse pro-T-cell cultures in which *TAL1* expression could be induced at a specific time point. For this, pro-T cells were derived from CreER-recombinase transgenic mice and cultured in the presence of Scf, Il7 and immobilized Dll4, as described previously[18] (Figure 4A). These pro-T cells were transduced with inducible retroviral vectors containing either *TAL1*, *AKT^{E17K}* or *TAL1+AKT^{E17K}* cloned in the antisense orientation between mutant LoxP sites to make the expression inducible[19] (Figure 4B). Green fluorescent protein (GFP) was constitutively expressed from these vectors, while blue fluorescent protein (BFP) was expressed together with *TAL1* or *AKT^{E17K}*, but no additional fluorescent protein was present when both *TAL1* and *AKT^{E17K}* were co-expressed (Figure 4B). Different treatment conditions with 4OH-tamoxifen were tested to determine the best recombination efficiency (*Online Supplementary Figure 3A*). Treatment of these cells with 1 μM 4OH-tamoxifen successfully induced inversion of the DNA between the mutant LoxP sites resulting in the expression of the inserted cDNA (*Online Supplementary Figure 3B*).

Induced expression of *TAL1* (determined by BFP expression) led to a selective growth disadvantage with the percentage of *TAL1* expressing pro-T cells decreasing over time (Figure 4C). This growth disadvantage could be overcome by constitutive expression of *AKT^{E17K}* (+mCherry) in the pro-T cells. The *AKT^{E17K}* + *TAL1* double positive pro-T cells became the major clone over time in these cultures (determined by BFP and mCherry expression) (Figure 4C).

In order to further characterize this negative effect of *TAL1* expression and the rescue by AKT pathway activation, we generated isogenic pro-T cells with inducible expression of *TAL1*, *AKT^{E17K}* or *TAL1+AKT^{E17K}* and followed these cultures in the presence or absence of induction by absolute cell counts. Induction of *TAL1* caused again a growth disadvantage as cell numbers were lower than in uninduced cells (Figure 4D). Induced expression of *AKT^{E17K}* provided a growth advantage to the cells and induction of *TAL1+AKT^{E17K}* provided an even stronger growth advantage, indicating that *TAL1* expression cooperated with *AKT^{E17K}* to drive stronger proliferation in these pro-T cell cultures (Figure 4D). Furthermore, pro-T-cells expressing *TAL1+AKT^{E17K}* showed IL7 independent growth with also here *TAL1+AKT^{E17K}* double positive cells becoming the predominant clone over time (Figure 4E).

In order to verify that *Pten* inactivation had similar effects compared to *AKT^{E17K}*, we also repeated these experiments using pro-T cells derived from Cas9 transgenic mice and

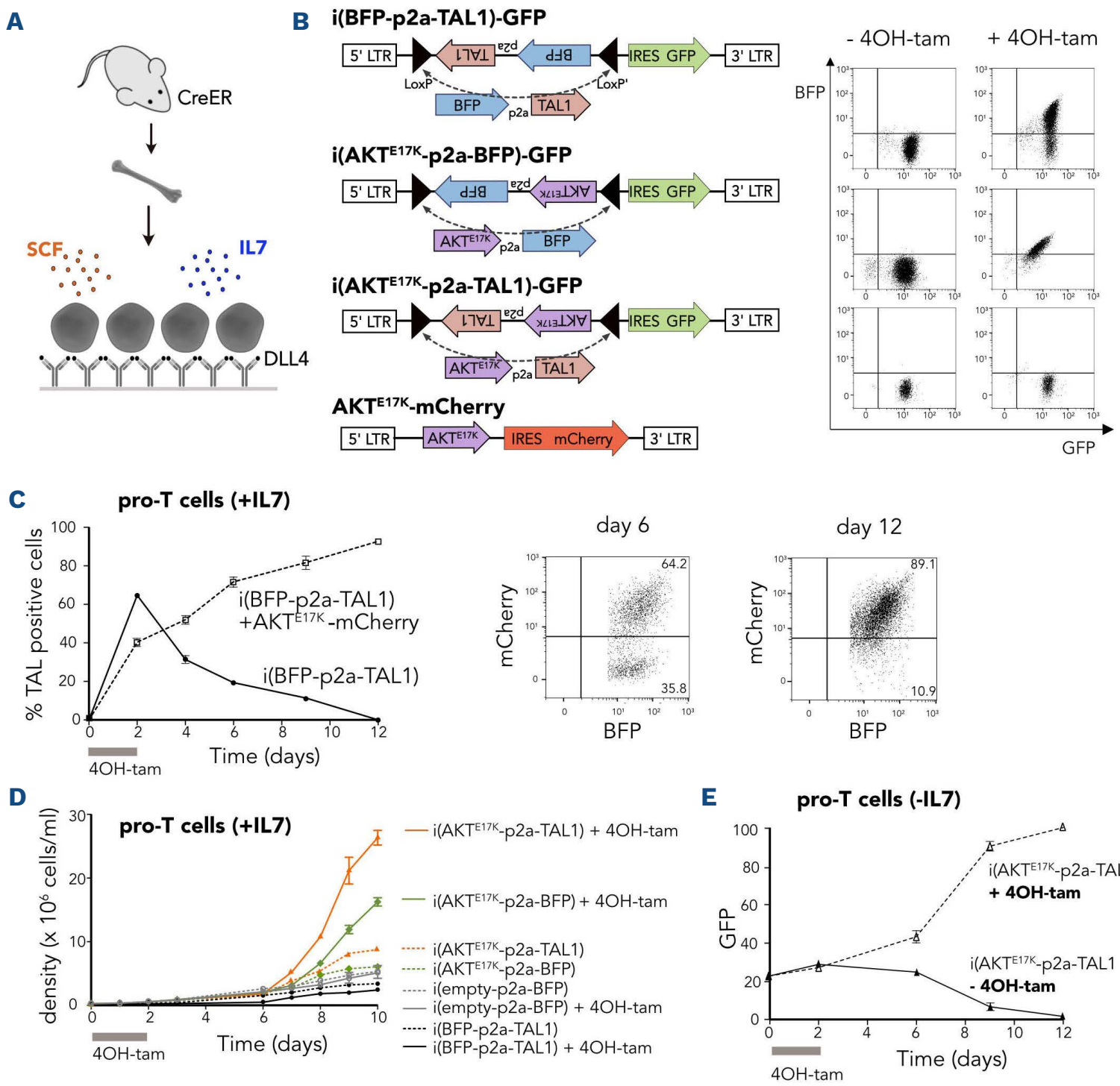

Figure 4. *TAL1* expressing pro-T cells show a growth disadvantage, which can be rescued by co-expressing mutant AKT. (A) Scheme of *ex vivo* pro-T-cell culture derived from Cre-ER mice, requiring interleukin-7 (IL7), stem cell factor (SCF) and immobilized Delta-like ligand 4 (DLL4) for proliferation. (B) Pro-T cells were transduced with inducible retroviral constructs for expression of *TAL1*, *AKT^{E17K}* or *TAL1+AKT^{E17K}*. Pro-T cells were sorted for green fluorescent protein (GFP) and treated with 1 mM 4-OH tamoxifen for 48 hours to activate Cre-ER and induce LoxP-mediated inversion and expression of the oncogenes. Constructs having *TAL1* and *AKT^{E17K}* become blue fluorescent protein (BFP)-positive, indicating the construct has successfully flipped. The construct containing both *TAL1* and *AKT^{E17K}* does not contain BFP. (C) The percentages of each population in pro-T cells having *TAL1* or *TAL1+AKT^{E17K}* were followed over time (BFP) cells when co-expression with mutant AKT (mcherry). Co-transduced cells in which the constructs were flipped become the largest population (BFP + mcherry). (D) Cell densities (mean +/- standard deviation) over time for different proT-cells conditions. (E) Cell densities (mean with standard deviation), as measure of absolute proliferation, were measured over time for different pro-T cell conditions: *TAL1*, *AKT^{E17K}*, *TAL1+AKT^{E17K}* and WT empty control. F, *TAL1-AKT^{E17K}* expressing pro-T cells were able to grow in the absence of IL7.

we inactivated *Pten* via retroviral transduction of a Pten targeting gRNA. These cells showed again the *TAL1* growth disadvantage, which could be rescued by *Pten* inactivation (*Online Supplementary Figure S3C*).

Palamarchuk *et al*. showed that the TAL1 protein can be phosphorylated by AKT at a threonine residue at position 90, leading to inhibition of its repressor activity.[31] In order to test whether via this mechanism TAL1 growth disadvantage can be rescued, we performed polymerase chain reaction (PCR) mutagenesis to create TAL1^{T90A} and TAL1^{T90D} mutants. TAL1^{T90D} would mimic the phosphorylated form of TAL1, while TAL1^{T90A} would prevent phosphorylation and mimic the unphosphorylated form of TAL1. However, growth of the pro-T cells was still negatively affected by TAL1^{T90D} or TAL1^{T90A} and their survival could still be rescued by AKT^{E17K}. Both observations indicate that phosphorylation of TAL1 by AKT at Thr90 is not the major mechanism of cooperation (*Online Supplementary Figure 3D*).

TAL1 induces growth disadvantage by upregulating pro-apoptotic genes

When performing a constitutive bone marrow transplantation with *TAL1* compared to empty vector, we observed that when *TAL1* was constitutively expressed in the absence of AKT signaling, the *TAL1*-positive cells were initially engrafted, but showed lower numbers in bone marrow and blood compared to empty vector and were slowly disappearing over time (Figure 5A), indicating that *TAL1* cannot induce leukemia on its own, and could even be a negative factor suppressing hematopoietic growth. In order to get insight in the mechanism of *TAL1*-induced growth disadvantage and rescue mechanism of PI3K-AKT pathway hyperactivation we performed gene expression profiling on *TAL1* expressing pro-T cells and on *TAL1* transduced T cells from the mouse model and in *TAL1+AKT^{E17K}* lymphoma cells.

We used the inducible *TAL1* expression in the pro-T cells to extract RNA on different times points after induction. Pro-T cells with induced *TAL1* expression were sorted for GFP and RNA was extracted at 0, 6, 12, 18 and 24 h after treatment with 1 µM 4OH tamoxifen (Figure 5B). Expression of TAL1 was confirmed by western blotting (Figure 5C). Six hours after induction of *TAL1* expression there was no significant difference in gene expression compared to uninduced cells, but at 12 h of induction the first gene expression changes were observed that were further enhanced at 18 and 24 h after induction (Figure 5D). At time point 18 h and 24 h there was upregulation of known *TAL1* target genes such as *Runx1* and *Gata3*, as well as strong signatures of E2f target genes and Myc target genes. In agreement with immunophenotype of TAL1+AKT^{E17K} thymic cells, a significant upregulation of *IL2ra* (CD25) was observed at all time points.

Interestingly, at 18 h and 24 h after induction of *TAL1* there was upregulation of cell-cycle and proliferation markers (upregulation of *Cdk1*, *Hes1*, *Nmyc*, *Mki67*; downregulation of

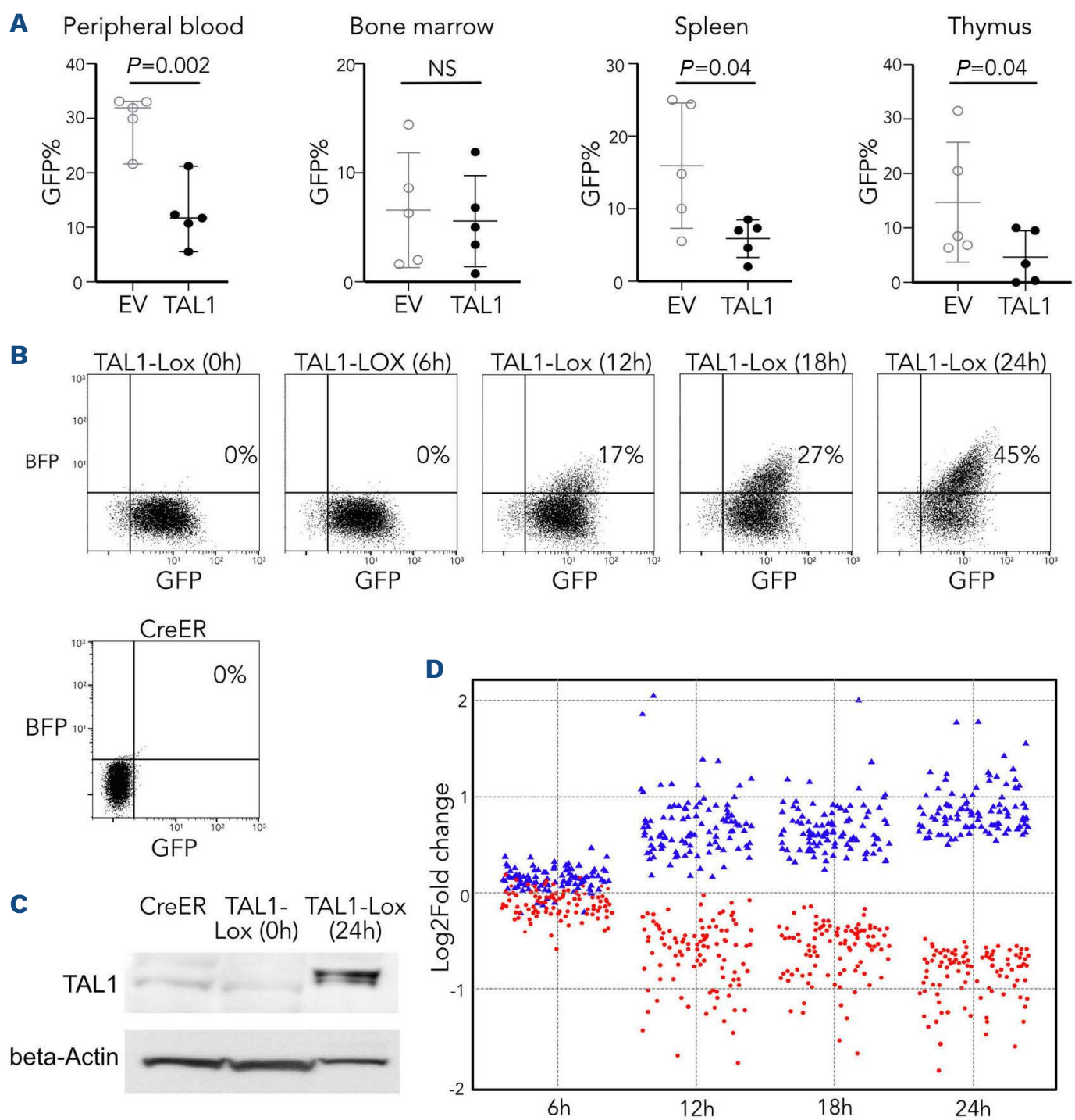

Continued on following page.

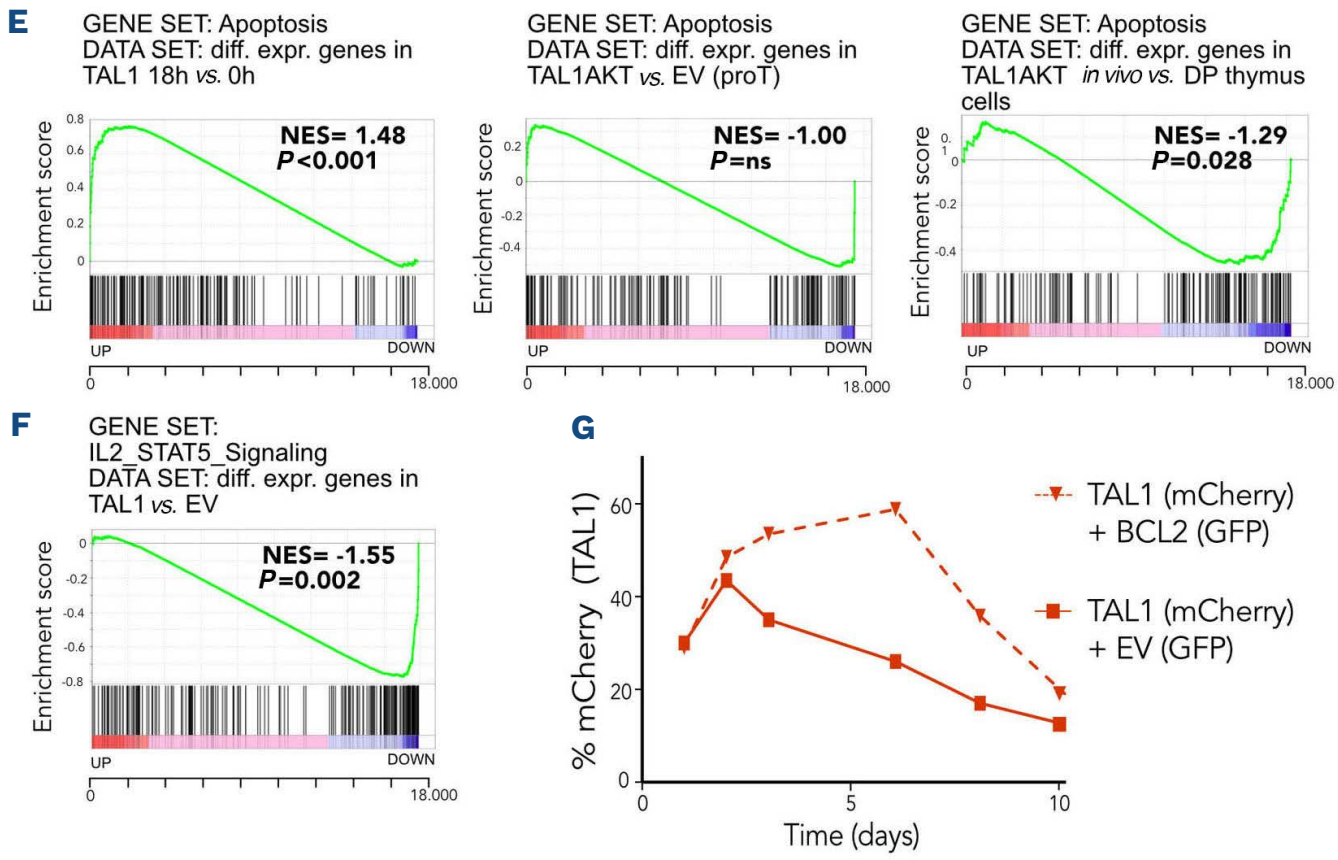

Figure 5. *TAL1* induces a growth disadvantage *in vitro* by direct upregulation of apoptosis. (A) Plots showing percentage green fluorescent protein (GFP)-positive cells in peripheral blood, bone marrow, spleen and thymus at time of sacrifice: *TAL1*-positive *vs.* empty vector cells. *P*-values were calculated using unpaired *t*-test. (B) CreER pro-T cells were transduced with *TAL1*-inducible constructs, which were sorted for GFP. Next these cells were cultured in presence of 4OH tamoxifen. Successful flipping of the construct is seen over time as blue fluorescent protein (BFP) signal increases over time. RNA extraction was performed on indicated time points. (C) At 48 hours (h) cells were sorted for BFP and expression of TAL1 was confirmed by western blot. (D) Representation of the 100 most up- and downregulated genes at 24 h compared to 0 h over time. (E) Gene set enrichment analysis (GSEA) showing significantly positive enrichment of pro-apoptotic genes after *TAL1* induction compared to non-treated pro-T cells. NES: normalized enrichment score; *P*: nominal *P*-value. (F) GSEA showing significantly negative enrichment of IL2-STAT5 signaling in *TAL1*-positive thymus cells compared to empty vector (EV) thymus cells. NES: normalized enrichment score; *P*: nominal *P*-value. (G) Growth curve showing percentage of *TAL1*-positive (mcherry positive) cells over time.

Rb1, *Pten*), but at the same time also a significant enrichment for apoptotic genes, including upregulation of several pro-apoptotic caspases (Figure 5E; *Online Supplementary Figure S4*). In contrast, *AKT*^{E17K} and *TAL1+AKT*^{E17K} expressing pro-T cells showed no or negative enrichment of apoptosis genes, suggesting that *AKT*^{E17K} can counteract *TAL1*-induced apoptosis (Figure 5E). RNA-sequecing analysis of sorted *TAL1*-positive T cells harvested from the thymus of the *in vivo* mouse models showed strong downregulation of IL7-JAK-STAT pathway genes with *Bcl2* and IL7 receptor genes as most significantly downregulated genes (Fig. 5F). In order to confirm the role of apoptosis in *TAL1* induced growth disadvantage, we overexpressed Bcl2 in pro-T cells expressing *TAL1*. Expression of *Bcl2* allowed the *TAL1*-expressing cells to grow initially and the growth retardation was now clearly delayed, indicating that apoptosis was at least partially responsible for the observed negative effect of *TAL1* (Figure 5G).

These data indicate that *TAL1* expression can both induce pro-proliferation and pro-apoptosis effects and that its oncogenic characteristics can only become evident in the right signaling background such as in the presence of strong AKT signaling.

TAL1-AKT^{E17K} leukemic cells are more sensitive to PI3K inhibitors

Based on our data that *TAL1* expression in the absence of strong AKT signaling is having a negative effect on cell survival, we hypothesized that PI3K/AKT pathway inhibition in *TAL1*-positive T-ALL cells could elicit a stronger anti-leukemia effect compared to *TAL1*-negative cells. In order to study this, we tested if *TAL1+AKT*^{E17K} transformed pro-T cells were more sensitive to PI3K-AKT inhibition compared to *AKT*^{E17K} transformed pro-T cells. These transformed pro-T cells were cultured in multi-well plates and treated with increasing concentrations of Dactolisib or MK2206, respectively a potent PI3K-mTOR and AKT inhibitor (Figure 6A). Both *TAL1+AKT*^{E17K} and *AKT*^{E17K} transformed pro-T cells were sensitive to these inhibitors and the *TAL1+AKT*^{E17K} expressing cells were clearly more sensitive with an half maximal inhibitory concentration (IC50) value >10-times lower than *AKT*^{E17K} transformed pro-T cells (Figure 6A).

Similarly, we also treated thymic cells derived from the *TAL1+AKT*^{E17K} and *AKT*^{E17K} mouse lymphoma/leukemia models (Figure 6B). Cells were cultured for short term *ex vivo* and treated for 24 h with either Dactolisib or MK2206. In both conditions, cells were very sensitive to PI3K inhibitors com-

pared to wild-type thymic cells and *TAL1+AKT*^{E17K} thymic cells were about three-times more sensitive to MK2206 compared to *AKT*^{E17K} expressing cells ($P<0.001$), while this difference was not significant for dactolisib ($P=0.09$) due to more variability in the growth of the primary cells (Figure 6B).

Together, these data from the mouse lymphoma/leukemia cells and the pro-T cells clearly indicate that *TAL1+AKT*^{E17K} transformed cells are more sensitive to PI3K/AKT pathway inhibition compared to *AKT*^{E17K} transformed cells, illustrating the negative impact of *TAL1* expression in the absence of PI3K-AKT signaling.

TAL1-AKT positive cells upregulate DNA repair genes and show increased sensitivity to PARP inhibitors

Expression analysis of *TAL1* positive pro-T cells (Figure 7A) and *TAL1* expressing thymic cells (Figure 7B) showed that *TAL1* expression was associated with an enrichment of genomic instability markers. Interestingly, there was also positive enrichment for DNA repair and *TP53* pathway genes in human T-ALL samples with *TAL1* expression and PI3K-AKT pathway mutations, indicating that the subgroup of *TAL1* positive T-ALL cases with PI3K-AKT pathway mutations could have increased dependency on DNA repair genes compared to other T-ALL cases (Figure 7C). *TAL1*-expressing cells had an upregulation of DNA repair genes and downregulation of genes involved with the response to UV induced damage (Figure 7D). There was upregulation of genes in each of the DNA repair pathways including non-homologous end joining, homologous end joining, base excision repair and nucleotide excision repair and the strongest association was observed with nucleotide excision repair (NER) (Figure 7E), which is a DNA repair mechanism for single stranded DNA breaks involving PARP1. In agreement with this, publicly available data from the CancerRx data set revealed sensitivity of JURKAT, a *TAL1*-positive T-ALL cell line, for the PARP1 inhibitor Olaparib. Together, these data suggest that *TAL1* expression and PI3K-AKT pathway activation might sensitize cells towards PARP1 inhibition.

In order to investigate this further, we used the pro-T cell model with *AKT*^{E17K} or *TAL1+AKT*^{E17K} and compared the sensitivity of these cells to empty vector transduced pro-T cells. Empty vector transduced pro-T cells were not very sensitive to Olaparib (Figure 7F). There was also no synergy detected between Olaparib and Dactolisib in the normal

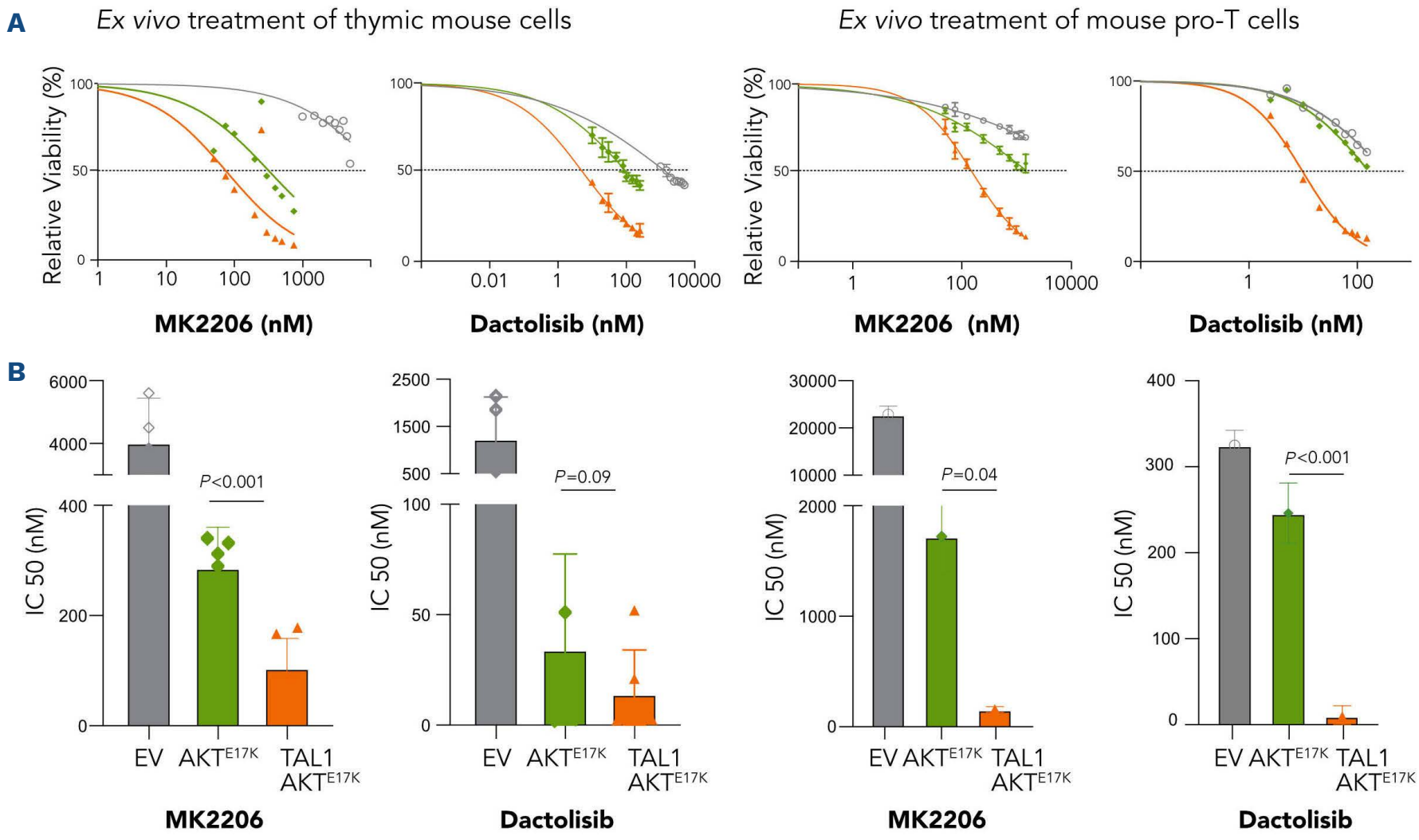

Figure 6. *TAL1-AKT*^{E17K} pro-T and leukemic cells are more sensitive to PI3K inhibition compared to AKT^{E17K} only cells. (A) Dose response curves showing relative (to dimethyl sulfoxide [DMSO] concentration) viability of leukemic cells in response to 24 hours of treatment with increasing concentrations of PI3K-mTOR inhibitor Dactolisib and AKT inhibitor MK2206. Thymic mouse cells (left): m267 (AKT^{E17K}), m271 (TAL1+AKT^{E17K}) and Cas9 pro-T cells (right). (B) Bar plots showing half maximal inhibitory concentration (IC50) values for different Leukemic cells/ pro-T cell conditions treated with PI3k-mTOR inhibitor Dactolisib and AKT inhibitor MK2206. *P*-values were calculated using the one-way ANOVA with Tukey correction to account for multiple comparisons.

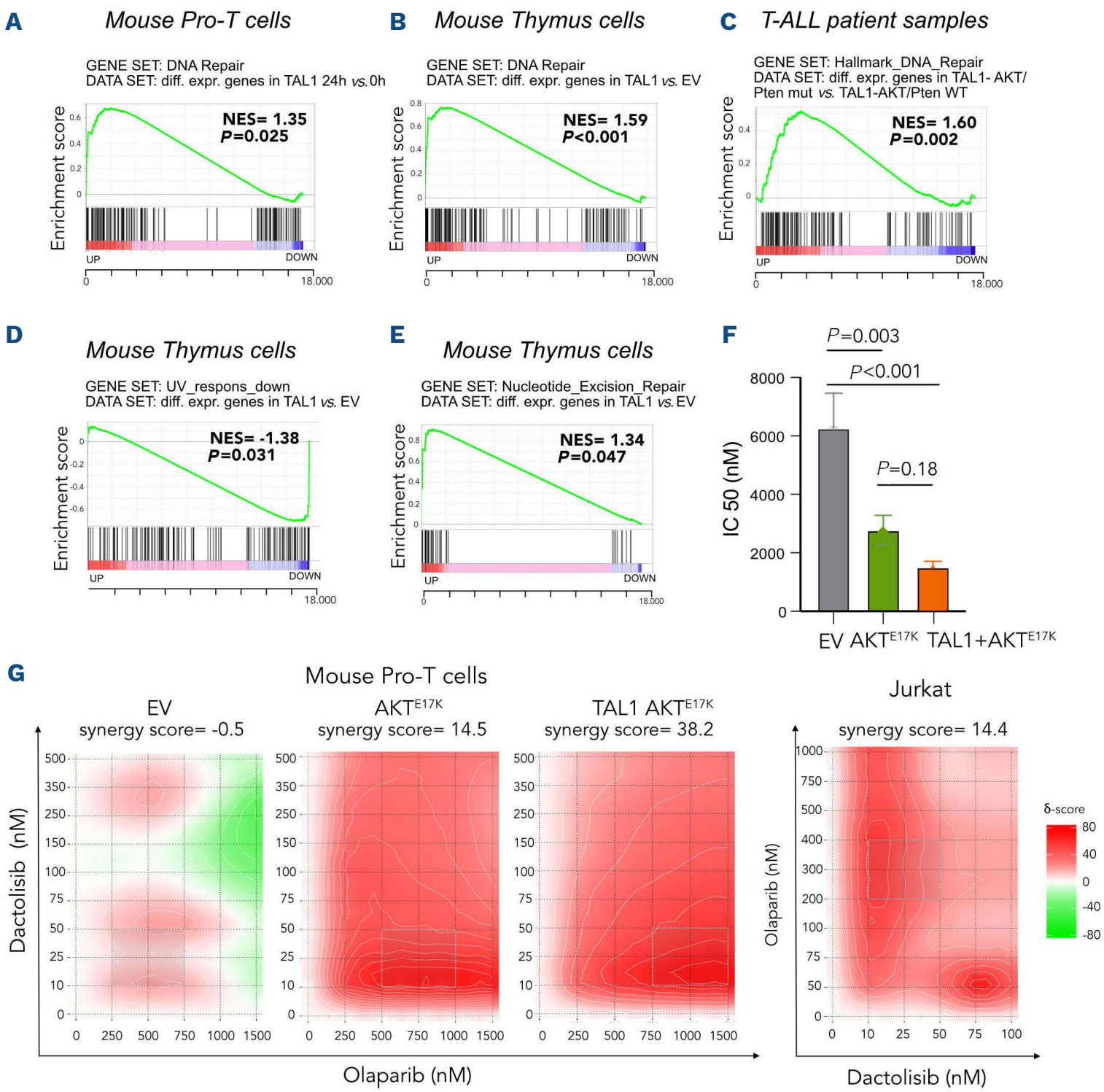

Figure 7. *TAL1* positive cells are characterized by a DNA repair signature and show increased sensitivity to PARP inhibitors. (A to C) Gene set enrichment analysis (GSEA) showing significant enrichment of DNA repair pathway in (A) *TAL1*-positive pro-T cells, (B) *TAL1*-positive thymus cells compared to empty vector (EV) thymus cells or (C) *TAL1* positive T-ALL with PI3K pathway activating mutations compared to *TAL1* T-ALL without mutations in PI3K pathway. NES: normalized enrichment score; *P*: nominal *P*-value. (D to E) GSEA showing significant negative enrichment of (D) UV response and positive enrichment of (E) nucleotide excision repair genes in *TAL1*-positive thymus cells compared to empty vector (EV) thymus cells. (F) Bar plots showing IC50 values for different pro-T cell conditions treated with PARP-inhibitor olaparib. *P*-values were calculated using the one-way ANOVA with Tukey correction to account for multiple comparisons. (G) Synergy matrix plots showing γ-scores for pro-T cells or Jurkat cells treated with dactolisib and olaparib (synergy score = the average γ-score for the whole range of concentrations shown in the synergy matrix).

pro-T-cell cultures (Figure 7G). Strikingly, both *AKT*^{E17K} and *TAL1+AKT*^{E17K} transformed pro-T cells showed sensitivity towards Olaparib and there was a strong synergy detected with Dactolisib that was more pronounced in cells transformed by *TAL1+AKT*^{E17K} compared to *AKT*^{E17K} alone (Figure 7F and G). Such synergy was also detected in JURKAT cells, a human T-ALL cell line with *TAL1* expression and AKT pathway activation (Figure 7G). These data in the isogenic pro-T cells clearly illustrate that *AKT*^{E17K} and *TAL1+AKT*^{E17K} transformed pro-T cells become dependent on PI3K/AKT signaling and become sensitive to PI3K/AKT pathway inhibitors, with the *TAL1+AKT*^{E17K} transformed cells being the most sensitive cells.

Discussion

TAL1 is a transcriptional regulator, that heterodimerizes with bHLH proteins such as E12, E47, HEB and E2-2 and is part of a large transcriptional complex with GATA1,

LMO1/LMO2 and Ldb1.[32-36] Some cases with *TAL1* expression also show increased *LMO1* or *LMO2* expression, explaining why previous mouse models for *TAL1* studies have focused on the cooperation between *TAL1* and *LMO1/2*. However, detailed RNA-sequencing analyses of T-ALL cases with *TAL1* expression indicates that only a minority of *TAL1* positive cases show increased *LMO1* or *LMO2* expression. In contrast, several studies have indicated that there is an overrepresentation of *PTEN* deletions and other mutations in the PI3K/AKT signaling pathway in *TAL1*-positive T-ALL.[5,16,17]

In this study we provide proof that *TAL1* expression and PI3K/AKT pathway activation indeed cooperate in driving T-ALL. We developed an inducible bone marrow transplant T-ALL model, where expression of *TAL1+AKT*^{E17K} leads to a transplantable leukemic disease whereas an *AKT*^{E117K} disease is not transplantable and *TAL1* alone does not generate any disease at all. These data indicate that AKT pathway activation in lymphoid progenitor cells is sufficient to activate proliferation and survival pathways, but that *TAL1* expression is required to induce stem cell properties and increase the number of leukemia initiating cells. Most importantly, these data clearly demonstrate that *TAL1* and PI3K-AKT pathway activation cooperate and drive leukemia development.

Interestingly, we find that both *in vivo* and *in vitro TAL1* expression in the absence of PI3K/AKT activation has a negative effect on cell growth. Pharmacologic inhibition of PI3K-AKT signaling showed pronounced anti-proliferative effects and induced apoptosis in pre-clinical models using leukemia cell lines or primary leukemia samples.[37-41] Given the negative effect of *TAL1* on cell growth and the key role of PI3K signaling in *TAL1*-positive T-ALL, we examined the effect of PI3K-AKT inhibitors in our different models. In agreement with the negative effect of *TAL1* on cell growth, we show that inactivation of PI3K/AKT pathway has a stronger effect on viability in *TAL1+AKT*^{E17K} cells compared to AKT cells. These findings have potentially important therapeutic potential, as we demonstrate that *TAL1+AKT*^{E17K} cells are highly sensitive to AKT pathway inhibition, more sensitive than expected due to the negative effects of *TAL1* on T-cell survival in the absence of AKT pathway activation. With several PI3K/AKT pathway inhibitors in development,[37-41] these data could find clinical applications for high risk T-ALL patients with PI3K/AKT pathway activation in whom stardard treatment does not lead to MRD negativity. Dactolisib (BEZ235) is a dual pan-PI3K and mTOR inhibitor for which a phase I study in acute leukemia showed positive effect in a subset of ALL patients.[39] However, digestive toxicity (mostly dose-dependent) remains an important problem. MK2206, an allosteric pan-AKT inhibitor, has been shown to induce apoptosis and autophagy in T-ALL cell lines and primary patient samples.[40] Phase II clinical studies in refractory lymphomas have shownd a favorable safety profile.[41]

The role of poly (ADP-ribose) polymerases (PARP) in malignancy is well known in BRCA1/2 mutant tumors known to be deficient in homologous recombination mechanisms.[42] Mutations in BRCA1/2 genes are uncommon in hematological cancers, but data have shown that the clinical benefits of PARP inhibition are not restricted to BRCA mutant cancers.[42,43] In our study we found enrichment of DNA repair genes in *TAL1*-positive T-ALL patients with PI3K pathway compared to *TAL1*-positive T-ALL patients without PI3K hyperactivation, suggesting a role for PI3K pathway in DNA repair. Furthermore, our RNA-sequencing data showed an upregulation of DNA repair in *TAL1*-positive pro-T cells and thymic mouse cells. Upregulation of DNA repair is a known mechanism of cancer cells to maintain oncogenic growth and chemoresistance and to protect the cells from DNA damage. Our data thus indicated that both *TAL1* expression and PI3K-AKT pathway activation could increase the dependency on DNA repair mechanisms. Indeed, AKT^{E17K} and TAL1+AKT^{E17K} pro-T cells are much more sensitive to PARP inhibition compared to control pro-T cells. Moreover, when combining Olaparib with Dactolisib, synergy was observed in AKT^{E17K} and TAL1-AKT^{E17K} transformed cells with the strongest synergy in TAL1-AKT^{E17K} transformed cells.

In conclusion, we demonstrate direct cooperation between *TAL1* and PI3K/AKT pathway signaling to drive T-ALL development using *ex vivo* T-cell cultures and a novel *in vivo* mouse model. We identify *TAL1* as an apoptosis promoting factor in T cells in the absence of strong PI3K/AKT signaling, making *TAL1* positive T-ALL cells highly sensitive to PI3K/AKT pathway inhibition. Moreover, we find that both *TAL1* and PI3K/AKT induce a DNA repair signature in T-ALL and demonstrate that PARP inhibitors may be attractive therapeutic agents in combination with PI3K inhibitors in *TAL1*-positive T-ALL.

Disclosures

No conflicts of interest to disclose.

Contributions

NT, NM, OG, SP performed experiments. NT, SD, JC designed experiments, analyzed data and wrote the paper.

Funding

NT holds a fellowship of the FWO-Vlaanderen. SD holds a fellowship of the Foundation Against Cancer. This work was funded by a grant from FWO-Vlaanderen (to JC).

Data-sharing statement

All RNA-seq data have been deposited to Gene Expression Omnibus (GEO) with number GSE199823.

References

1. Raetz EA, Teachey DT. T-cell acute lymphoblastic leukemia. Hematology. 2016;2016(1):580-588.
2. Ferrando AA, Neuberg DS, Staunton J, et al. Gene expression signatures define novel oncogenic pathways in T cell acute lymphoblastic leukemia. Cancer Cell. 2002;1(1):75-81.
3. Soulier J, Clappier E, Cayuela J-M, et al. HOXA genes are included in genetic and biologic networks defining human acute T-cell leukemia (T-ALL). Blood. 2005;106(1):274-286.
4. Homminga I, Pieters R, Langerak AW, et al. Integrated transcript and genome analyses reveal NKX2-1 and MEF2C as potential oncogenes in T cell acute lymphoblastic leukemia. Cancer Cell. 2011;19(4):484-497.
5. Liu Y, Easton J, Shao Y, et al. The genomic landscape of pediatric and young adult T-lineage acute lymphoblastic leukemia. Nat Genet. 2017;49(8):1211-1218.
6. Girardi T, Vicente C, Cools J, De Keersmaecker K. The genetics and molecular biology of T-ALL. Blood. 2017;129(9):1113-1123.
7. Mansour MR, Abraham BJ, Anders L, et al. Oncogene regulation. An oncogenic super-enhancer formed through somatic mutation of a noncoding intergenic element. Science. 2014;346(6215):1373-1377.
8. Porcher C, Chagraoui H, Kristiansen MS. SCL/TAL1: a multifaceted regulator from blood development to disease. Blood. 2017;129(15):2051-2060.
9. Condorelli GL, Facchiano F, Valtieri M, et al. T-cell-directed TAL-1 expression induces T-cell malignancies in transgenic mice. Cancer Res. 1996;56(22):5113-5119.
10. Robb L, Rasko JE, Bath M L, Strasser A, Begley CG. Scl, a gene frequently activated in human T cell leukaemia, does not induce lymphomas in transgenic mice. Oncogene. 1995;10(1):205-209.
11. Ferrando AA, Herblot S, Palomero T, et al. Biallelic transcriptional activation of oncogenic transcription factors in T-cell acute lymphoblastic leukemia. Blood. 2004;103(5):1909-1911.
12. Larson RC, Lavenir I, Larson TA, Baer R, Warren AJ, Wadman I, et al. Protein dimerization between Lmo2 (Rbtn2) and Tall alters thymocyte development and potentiates T cell tumorigenesis in transgenic mice. EMBO J. 1996;15(5):1021-1027.
13. Tatarek J, Cullion K, Ashworth T, Gerstein R, Aster JC, Kelliher MA. Notch1 inhibition targets the leukemia-initiating cells in a Tal1/Lmo2 mouse model of T-ALL. Blood. 2011;118(6):1579-1590.
14. Tremblay M, Tremblay CS, Herblot S, et al. Modeling T-cell acute lymphoblastic leukemia induced by the SCL and LMO1 oncogenes. Genes Dev. 2010;24(11):1093-1105.
15. Gerby B, Tremblay CS, Tremblay M, et al. SCL, LMO1 and Notch1 reprogram thymocytes into self-renewing cells. PLoS Genet. 2014;10(12):e1004768.
16. Zuurbier L, Petricoin EF, Vuerhard MJ, et al. The significance of PTEN and AKT aberrations in pediatric T-cell acute lymphoblastic leukemia. Haematologica. 2012;97(9):1405-1413.
17. Mendes RD, Sarmento LM, Canté-Barrett K, et al. PTEN microdeletions in T-cell acute lymphoblastic leukemia are caused by illegitimate RAG-mediated recombination events. Blood. 2014;124(4):567-578.
18. Bornschein S, Demeyer S, Stirparo R, et al. Defining the molecular basis of oncogenic cooperation between TAL1 expression and Pten deletion in T-ALL using a novel pro-T-cell model system. Leukemia. 2018;32(4):941-951.
19. de Bock CE, Demeyer S, Degryse S, et al. HOXA9 cooperates with activated JAK/STAT signaling to drive leukemia development. Cancer Disc. 2018;8(5):616-631.
20. Gehre N, Nusser A, von Muenchow L, et al. A stromal cell free culture system generates mouse pro-T cells that can reconstitute T-cell compartments in vivo. Eur J Immunol. 2015;45(3):932-942.
21. Kim H, Kim M, Im S-K, Fang S. Mouse Cre-LoxP system: general principles to determine tissue-specific roles of target genes. Lab Anim Res. 2018;34(4):147-159.
22. Broux M, Prieto C, Demeyer S, et al. Suz12 inactivation cooperates with JAK3 mutant signaling in the development of T-cell acute lymphoblastic leukemia. Blood. 2019;134(16):1323-1336.
23. Hu Y, Smyth GK. ELDA: Extreme limiting dilution analysis for comparing depleted and enriched populations in stem cell and other assays. J Immunol Methods. 2009;347(1-2):70-78.
24. Lécuyer E, Hoang T. SCL: From the origin of hematopoiesis to stem cells and leukemia. Exp Hematol. 2004;32(1):11-24.
25. Aplan PD, Jones CA, Chervinsky DS, et al. An scl gene product lacking the transactivation domain induces bony abnormalities and cooperates with LMO1 to generate T-cell malignancies in transgenic mice. EMBO J. 1997;16(9):2408-2419.
26. Draheim KM, Hermance N, Yang Y, Arous E, Calvo J, Kelliher MA. A DNA-binding mutant of TAL1 cooperates with LMO2 to cause T cell leukemia in mice. Oncogene. 2011;30(10):1252-1560.
27. Chen B, Jiang L, Zhong ML, et al. Identification of fusion genes and characterization of transcriptome features in T-cell acute lymphoblastic leukemia. Proc Natl Acad Sci U S A. 2017;115(2):373-378.
28. Vicente C, Schwab C, Broux M, et al. Targeted sequencing identifies associations between IL7R-JAK mutations and epigenetic modulators in T-cell acute lymphoblastic leukemia. Haematologica. 2015;100(10):1301-1310.
29. Trinquand A, Tanguy-Schmidt A, Abdelali R ben, et al. Toward a NOTCH1/FBXW7/RAS/PTEN-based oncogenetic risk classification of adult T-Cell acute lymphoblastic leukemia: a group for research in adult acute lymphoblastic leukemia study. J Clin Oncol. 2013;31(34):4333-4342.
30. Tan SH, Yam AW, Lawton LN, et al. TRIB2 reinforces the oncogenic transcriptional program controlled by the TAL1 complex in T-cell acute lymphoblastic leukemia. Leukemia. 2016;30(4):959-962.
31. Palamarchuk A, Efanov A, Maximov V, Aqeilan RI, Croce CM, Pekarsky Y. Akt phosphorylates Tal1 oncoprotein and inhibits its repressor activity. Cancer Res. 2005;65(11):4515-4519.
32. Voronova AF, Lee F. The E2A and tal-1 helix-loop-helix proteins associate in vivo and are modulated by Id proteins during interleukin 6-induced myeloid differentiation. Proc Natl Acad Sci U S A. 1994;91(13):5952-5956.
33. O'Neil J, Shank J, Cusson N, Murre C, Kelliher M. TAL1/SCL induces leukemia by inhibiting the transcriptional activity of E47/HEB. Cancer Cell. 2004;5(6):587-596.
34. O'Neil J, Billa M, Oikemus S, Kelliher M. The DNA binding activity of TAL-1 is not required to induce leukemia/lymphoma in mice. Oncogene. 2001;20(29):3897-3905.
35. Valge-Archer VE, Osada H, Warren AJ, et al. The LIM protein RBTN2 and the basic helix-loop-helix protein TALl are present in a complex in erythroid cells. Proc Natl Acad Sci U S A. 1994;91(18):8617-8621.
36. Wadman IA, Osada H, Grü Tz GG, Agulnick AD, Westphal H, Forster A. The LIM-only protein Lmo2 is a bridging molecule assembling an erythroid, DNA-binding complex which includes

the TAL1, E47, GATA-1 and Ldb1/NLI proteins the GATA-1 gene in embryonal stem (ES) cells, which are The phenotypes of the. EMBO J. 1997;16(11):3145-3157.
37. Chiarini F, Grimaldi C, Ricci F, et al. Activity of the novel dual phosphatidylinositol 3-kinase/mammalian target of rapamycin inhibitor NVP-BEZ235 against T-cell acute lymphoblastic leukemia. Cancer Res. 2010;70(20):8097-8107.
38. Martelli AM, Evangelisti C, Chiarini F, McCubrey JA. The phosphatidylinositol 3-kinase/Akt/mTOR signaling network as a therapeutic target in acute myelogenous leukemia patients. Oncotarget. 2010;1(2):89-103.
39. Lang F, Wunderle L, Badura S, et al. A phase i study of a dual PI3-kinase/mTOR inhibitor BEZ235 in adult patients with relapsed or refractory acute leukemia. BMC Pharmacol Toxicol. 2020;21(1):70.
40. Simioni C, Neri LM, Tabellini G, et al. Cytotoxic activity of the novel Akt inhibitor, MK-2206, in T-cell acute lymphoblastic leukemia. Leukemia. 2012;26(11):2336-2342.
41. Oki Y, Fanale M, Romaguera J, et al. Phase II study of an AKT inhibitor MK2206 in patients with relapsed or refractory lymphoma. Br J of Haematol. 2015;171(4):463-470.
42. Pilié PG, Gay CM, Byers LA, O'Connor MJ, Yap TA. PARP inhibitors: extending benefit beyond BRCA-mutant cancers. Clin Cancer Res. 2019;25(13):3759-3771.
43. Fritz C, Portwood SM, Przespolewski A, Wang ES. PARP goes the weasel! Emerging role of PARP inhibitors in acute leukemias. Blood Rev. 2021;45:100696.